REPORT DOCUMENTATION PAGE

Form Approved
OMB No. 0704-0188

1. REPORT DATE *(DD-MM-YYYY)*
Mar 2014

2. REPORT TYPE
Briefing Charts

3. DATES COVERED *(From - To)*
Mar 2014- July 2014

4. TITLE AND SUBTITLE

Receptivity of a Cryogenic Coaxial Gas-Liquid Jet to Acoustic Disturbances

5a. CONTRACT NUMBER
In-House

5b. GRANT NUMBER

5c. PROGRAM ELEMENT NUMBER

6. AUTHOR(S)

Wegener, Forliti, Leyva, Talley

5d. PROJECT NUMBER

5e. TASK NUMBER

5f. WORK UNIT NUMBER
Q0YA

7. PERFORMING ORGANIZATION NAME(S) AND ADDRESS(ES)

Air Force Research Laboratory (AFMC)
AFRL/RQRC
10 E. Saturn Blvd
Edwards AFB CA 93524-7680

8. PERFORMING ORGANIZATION REPORT NO.

9. SPONSORING / MONITORING AGENCY NAME(S) AND ADDRESS(ES)
Air Force Research Laboratory (AFMC)
AFRL/RQR
5 Pollux Drive.
Edwards AFB CA 93524-7048

10. SPONSOR/MONITOR'S ACRONYM(S)

11. SPONSOR/MONITOR'S REPORT NUMBER(S)
AFRL-RQ-ED-VG-2014-174

12. DISTRIBUTION / AVAILABILITY STATEMENT
Distribution A: Approved for Public Release; Distribution Unlimited

13. SUPPLEMENTARY NOTES
Briefing Charts presented at 50th AIAA/ASME/SAE/ASEE Joint Propulsion Conference, Cleveland, OH, 28-30 July 2014. PA#14341

14. ABSTRACT
An experimental study has been conducted at the Air Force Research Laboratory at Edwards Air Force Base to explore the receptivity of cryogenic coaxial jet flows to transverse acoustic disturbances. The shear coaxial jet flow employed liquid nitrogen in the inner jet and cooled helium in the outer annular jet to represent the nominal fluid dynamical conditions of an oxygen/hydrogen liquid rocket engine injector. The injector flow is submerged in a chamber that experiences a monotonic transverse acoustic resonance characteristic of a rocket chamber in the presence of combustion instability. The coaxial jet is exposed to a variety of acoustic conditions including different frequencies, amplitudes, and locations within the resonant mode shape. High-speed back-lit images were captured to record the behavior of the natural (unforced) and forced coaxial jets. Proper orthogonal decomposition and spectral analysis were used to extract natural and forced modes. Convective modes are extracted, and a new Strouhal number is used to characterize the dominant natural convective mode that is analogous to the preferred mode in free jets. The threshold of receptivity was found for a number of different injector flows and acoustic forcing conditions. The results indicate that the dimensionless frequency plays an important role, and there exists a finite forcing amplitude at which the threshold of receptivity occurs. The receptivity threshold and post receptivity response provides useful insight on the suitability of a given injector design for specific rocket combustion chamber conditions.

15. SUBJECT TERMS

16. SECURITY CLASSIFICATION OF:			17. LIMITATION OF ABSTRACT	18. NUMBER OF PAGES	19a. NAME OF RESPONSIBLE PERSON
					Doug Talley
a. REPORT	**b. ABSTRACT**	**c. THIS PAGE**	SAR	25	**19b. TELEPHONE NO** *(include area code)*
Unclassified	**Unclassified**	**Unclassified**			661-275-6174

Standard Form 298 (Rev. 8-98)
Prescribed by ANSI Std. 239.18

Receptivity of a Cryogenic Coaxial Gas-Liquid Jet to Acoustic Disturbances

50th AIAA/ASME/SAE/ASEE Joint Propulsion Conference

Jeff Wegener, UCLA

David Forliti, Sierra Lobo, Inc.

Ivett Leyva, AFRL/RQRE

Doug Talley, AFRL/RQRC

Integrity ★ Service ★ Excellence

Public Affairs Clearance number xxxx

Outline

- Motivation and objectives
- Parameters of the forced coaxial jet
- Experimental facility
- Results
  - Unforced cases
  - Pressure node/antinode forcing
- Conclusions

Motivation: Combustion Instability in Rocket Engines

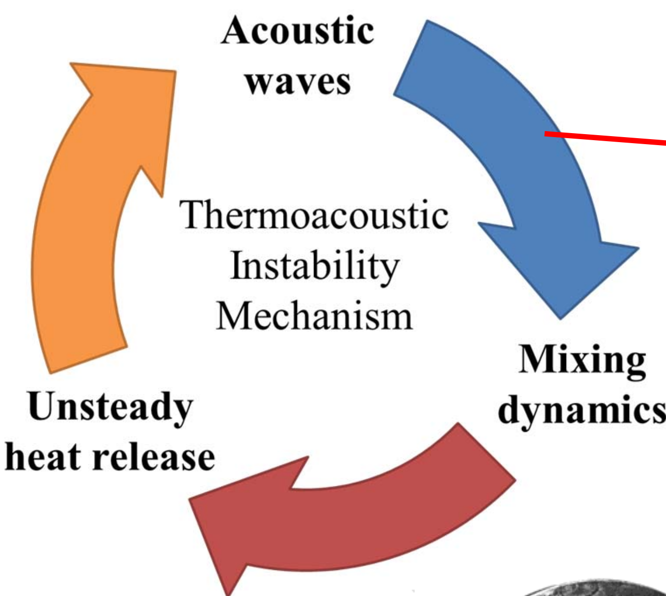

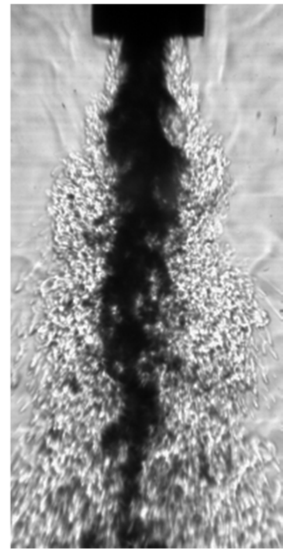

Objectives

Investigate acoustic receptivity characteristics of a model liquid rocket engine injector

- **Dimensionless frequency**
- **Acoustic amplitude**
- **Momentum flux ratio**
- **Location within the mode**

"Preferred mode" of the coaxial jet

- **Definition of natural frequency of the flow**
- **Characteristic velocity scale**

The Coaxial Jet

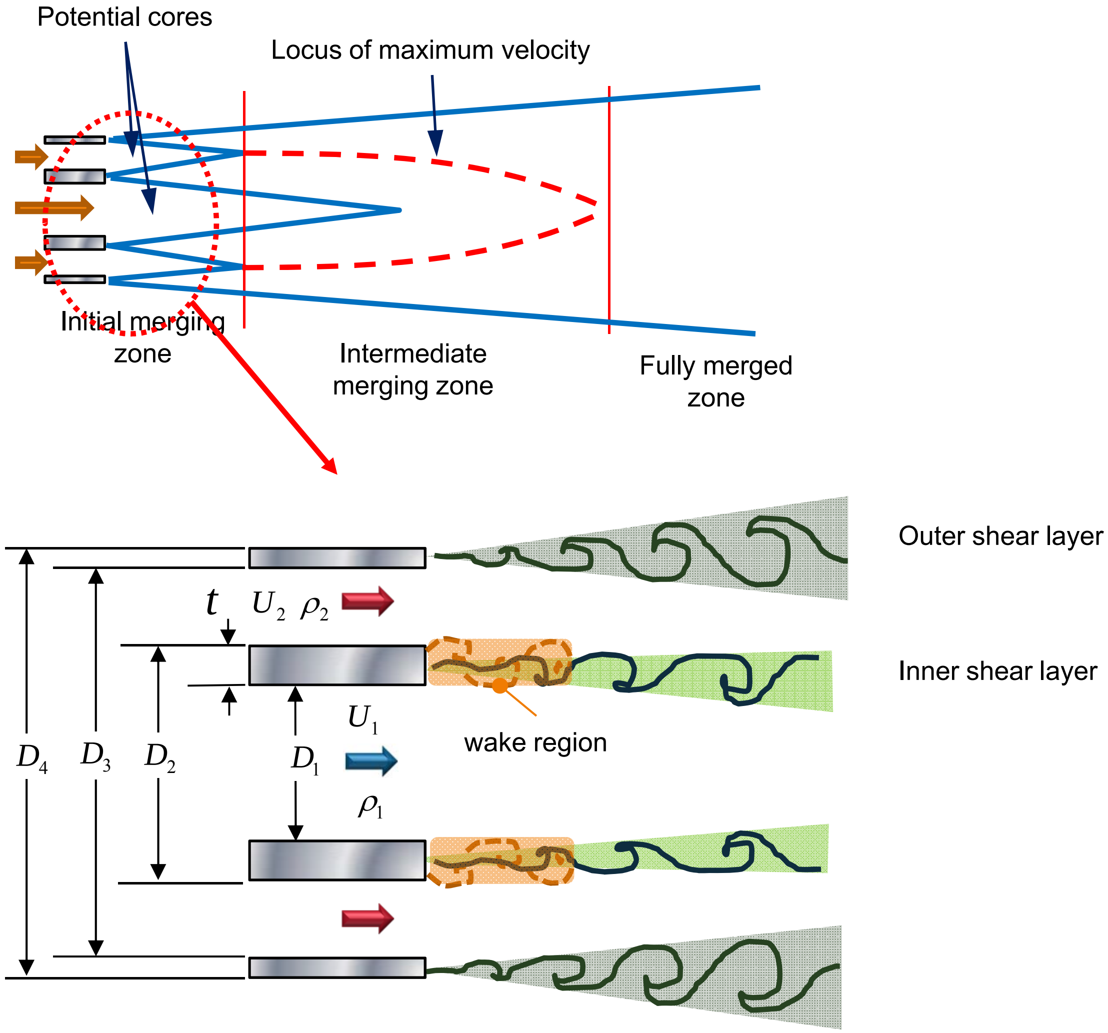

Geometry parameters

Area ratio

$$AR = \frac{D_3^2 - D_2^2}{D_1^2}$$

Dimensionless post thickness

$$\frac{t}{D_1}$$

Flow parameters

$$\mathrm{Re}_i = \frac{\rho_1 U_1 D_1}{\mu_1} \qquad \mathrm{Re}_i = \frac{\rho_2 U_2 (D_3 - D_2)}{\mu_2}$$

$$J = \frac{\rho_2 U_2^2}{\rho_1 U_1^2} \qquad r = \frac{U_2}{U_1} \qquad s_1 = \frac{\rho_2}{\rho_1} \qquad s_2 = \frac{\rho_3}{\rho_2}$$

$$We = \frac{\rho_2 U_2^2 D_1}{\sigma}$$

Inflow boundary conditions

- Mean velocity profiles
- RMS fluctuation profiles
- Spectral content

AFRL

The Forced Coaxial Jet

Very low density ratio regime: $0.005 < \frac{\rho_2}{\rho_1} < 0.1$

1. **Transverse Acoustic mode from chamber/siren**
   – f=f(c, geometry)
2. **Acoustic modes propellant lines**
   – f~c/2L
3. **Post wake**
   – $St=ft/U_{ch}$
4. **Shear layer instabilities**
   – $St_\theta=f\theta/U_{ch}$
5. **Jet preferred modes**
   – $St=fD_{ij}/U_{ij}$

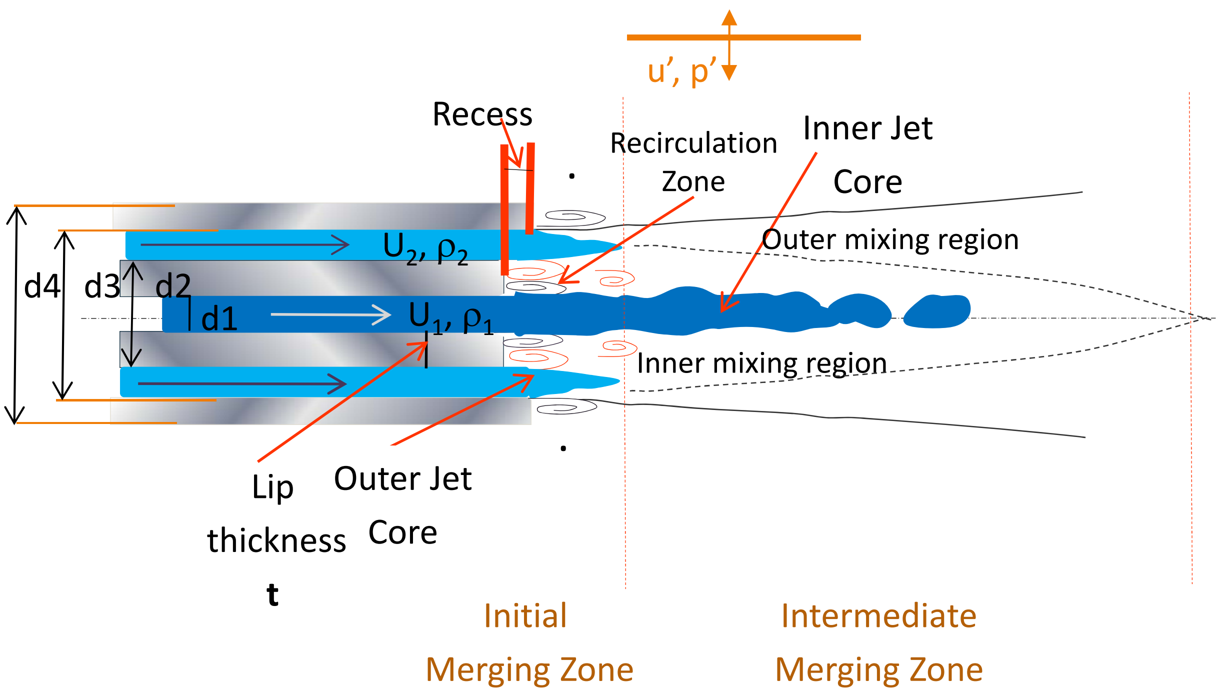

Forcing Characterization

- Shift pressure normalization from chamber pressure to injector dynamic pressure
- Normalize the frequency by the preferred mode of the coaxial jet
- Identify receptivity inception point—threshold for coupling between acoustics and flame

$$P'/\overline{P}_c \rightarrow \frac{P'}{\rho U^2/2} \qquad F = \frac{f_{forcing}}{f_{jet}}$$

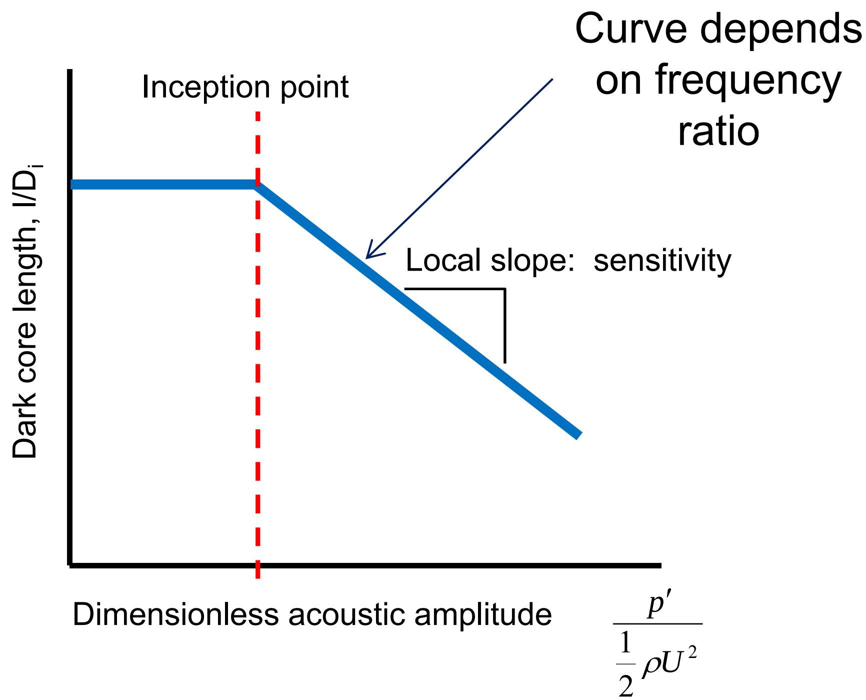

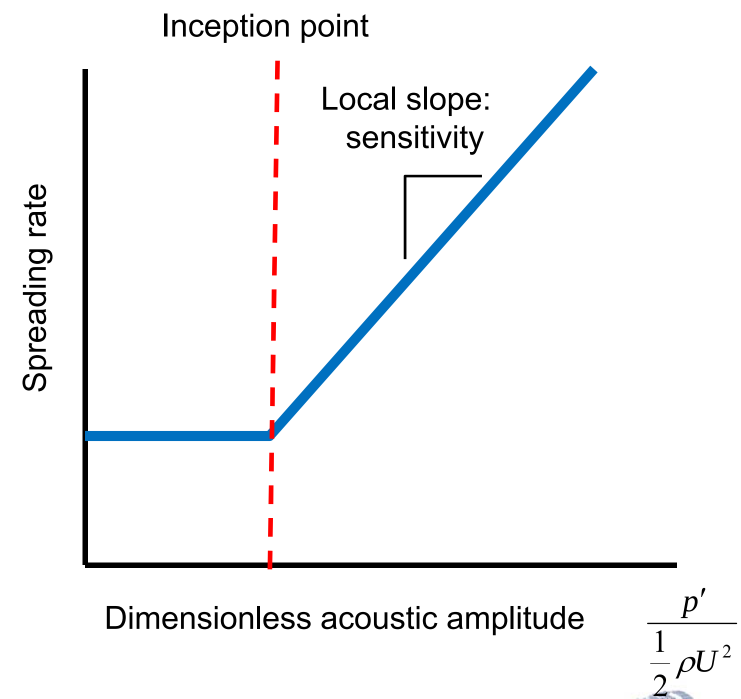

Experimental Facility

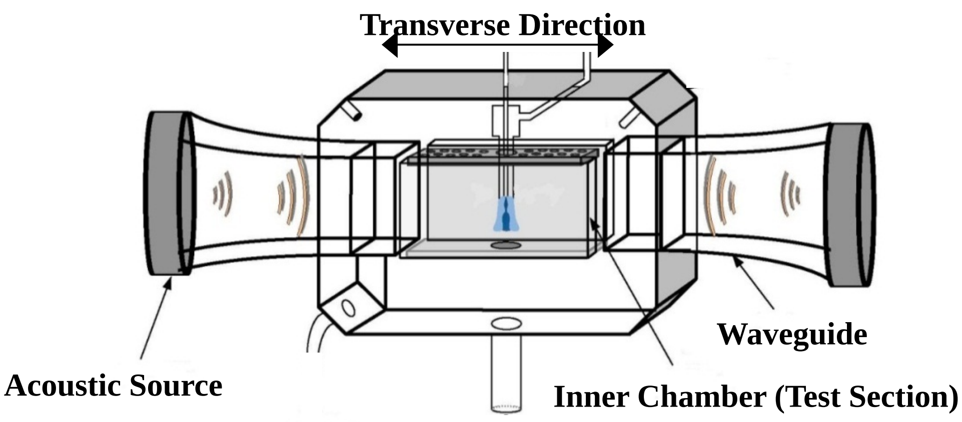

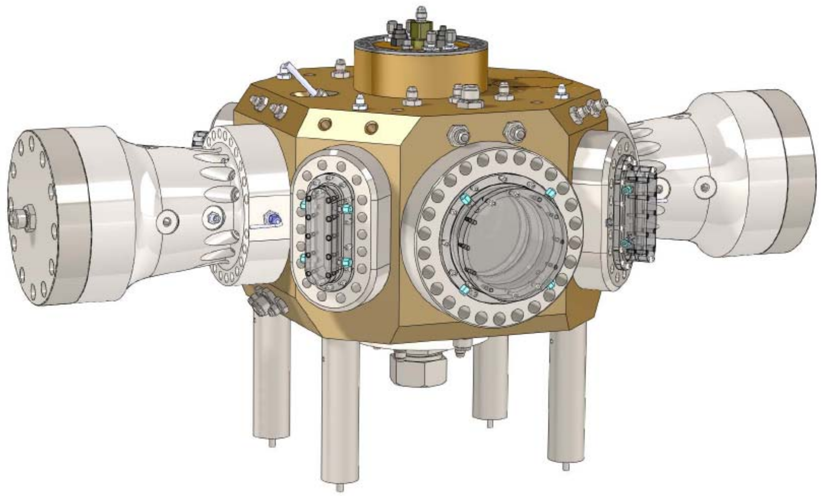

Capabilities

– Cryogenic propellant temperature control with high accuracy (±1 K)
– Sub- and super-critical chamber pressure (p_c up to 10.4 MPa)
– High amplitude acoustic forcing (p'/p_c ~ 0.02)
– Coaxial injector with extended length for fully developed turbulent flow (l_e/D > 110)
– High-speed diagnostic tools
  - Pressure transducer(s) natural frequency > 100 kHz
  - Time-series backlit imaging (f > 25 kHz)
  - Off-axis windows for future PIV/PLIF measurements

Experimental Conditions

- **New injector**
  - **D_1 = 1.4 mm**
  - **AR = 1.68**
  - **t/D_1 = 0.27**
- **J = 2 and 6**
- **N_2 inner jet @ 120 K**
- **Gaseous He @ 275 K**
- **$Re_1 \sim 1.5 \times 10^4$**
- **$Re_2 \sim 1 \times 10^4$**
- **Fully-developed turbulent flow conditions**
- **Chamber pressure 2.8 MPa (400 psi)→ subcritical**

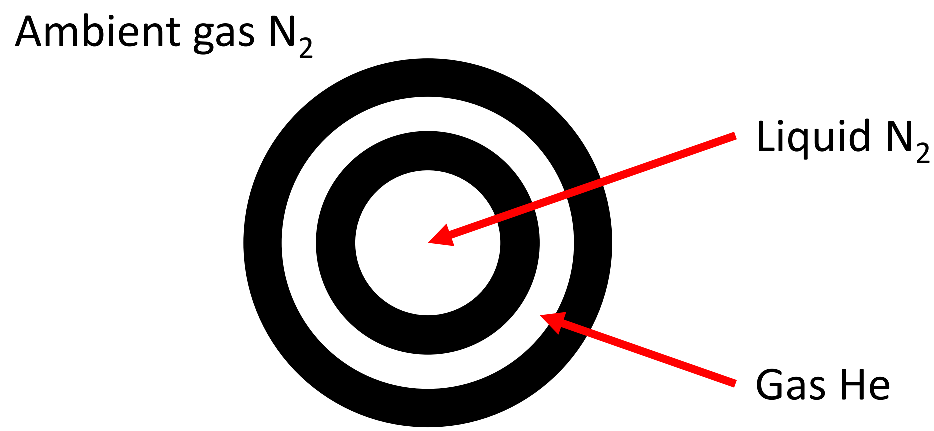

Unforced Cases

J = 2

J = 6

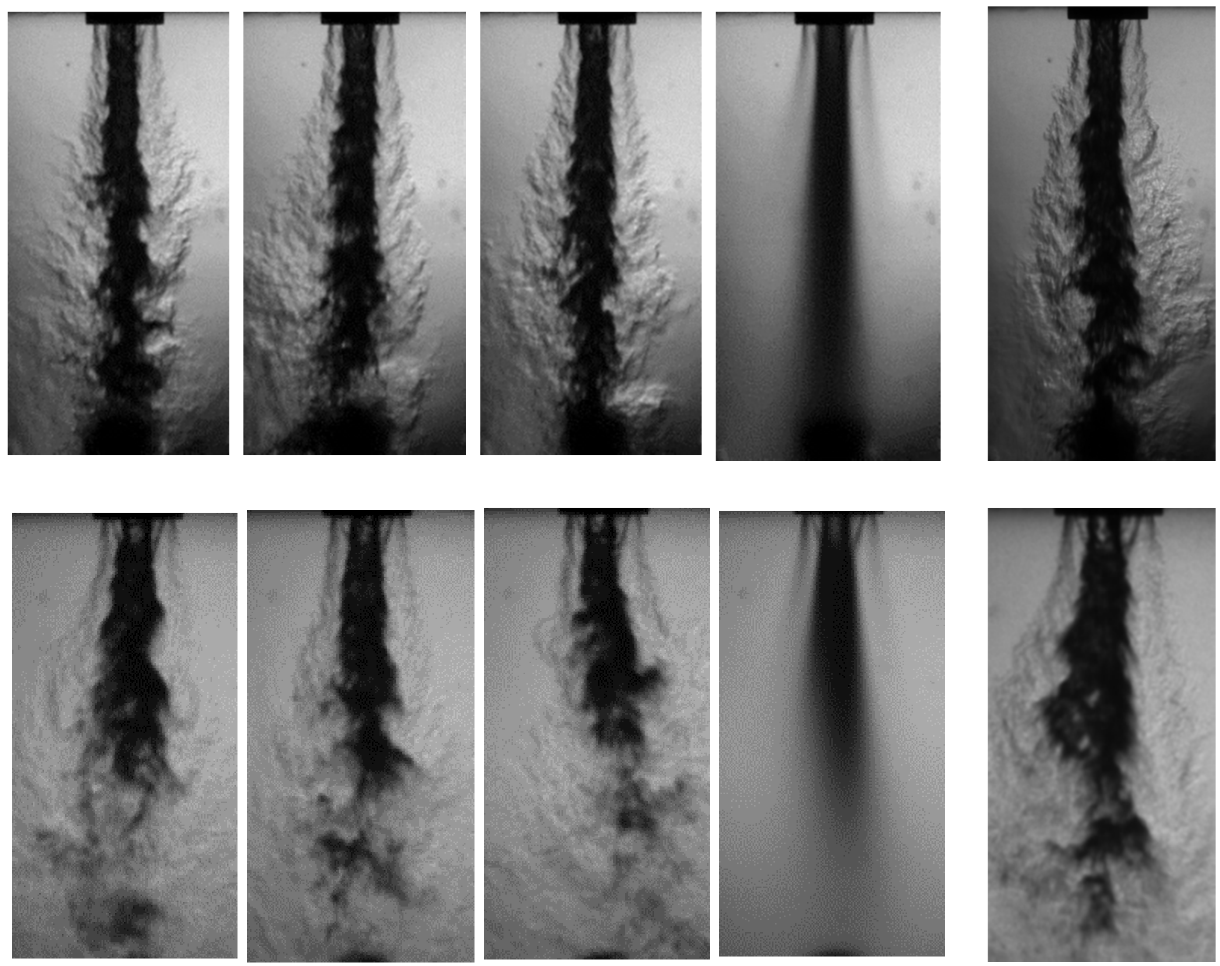

Convection Velocity

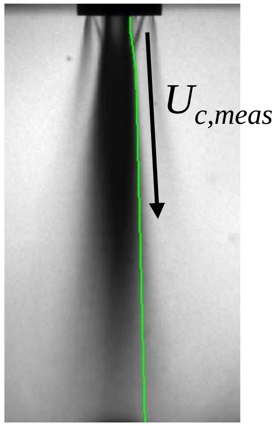

Verify the accuracy of the Dimotakis (1986) expression for shear layer convection velocity for these flow conditions.

$$U_{c,th} = \frac{U_o \rho_0^{1/2} + U_i \rho_i^{1/2}}{\rho_0^{1/2} + \rho_i^{1/2}}$$

$$U_{c,meas} = \frac{\Delta s}{\Delta t}$$

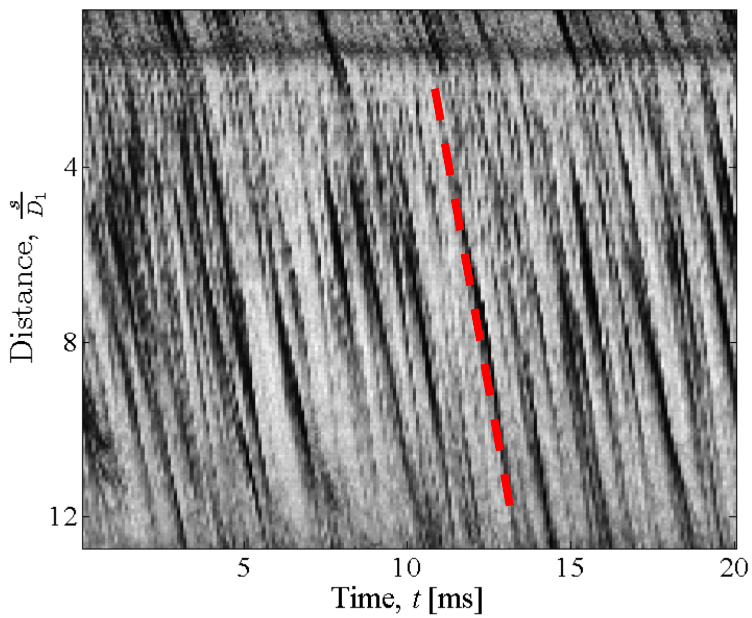

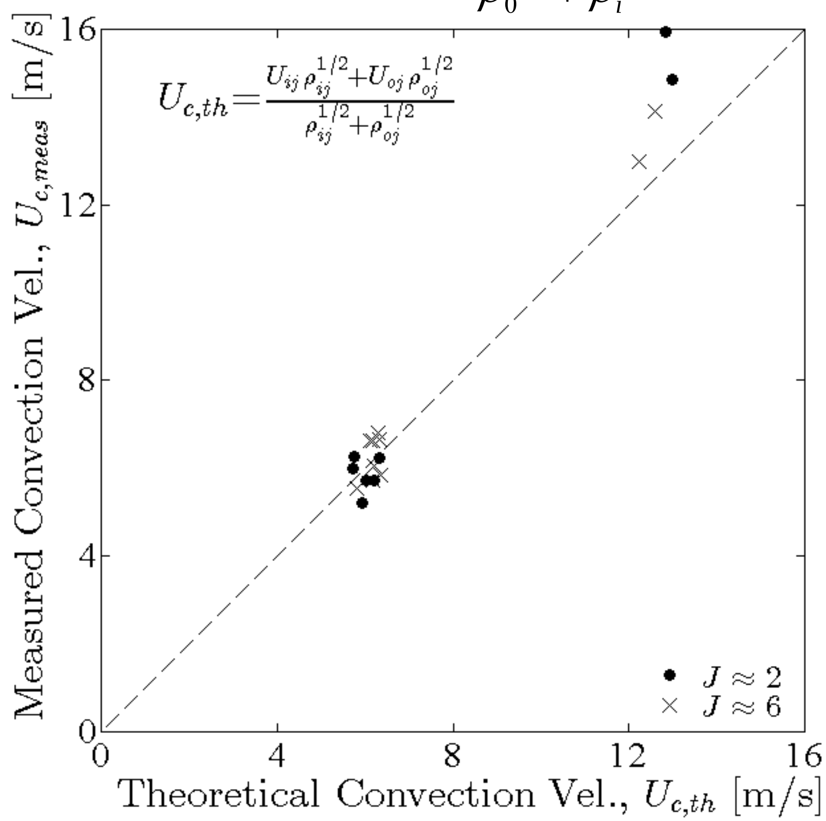

Preferred Mode Frequency

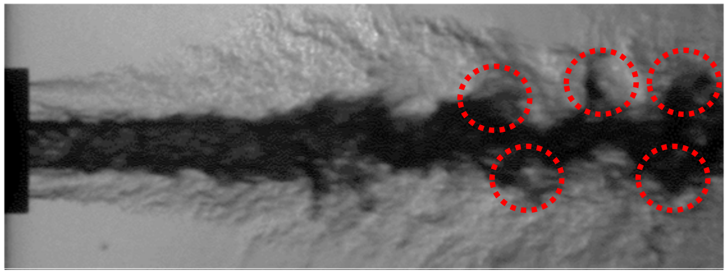

Most energetic convective mode pair from POD

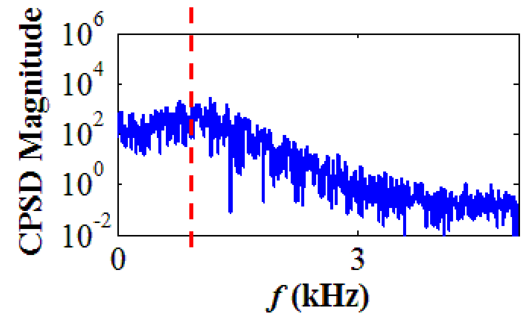

Previous injectors (Sophonias, 2012)

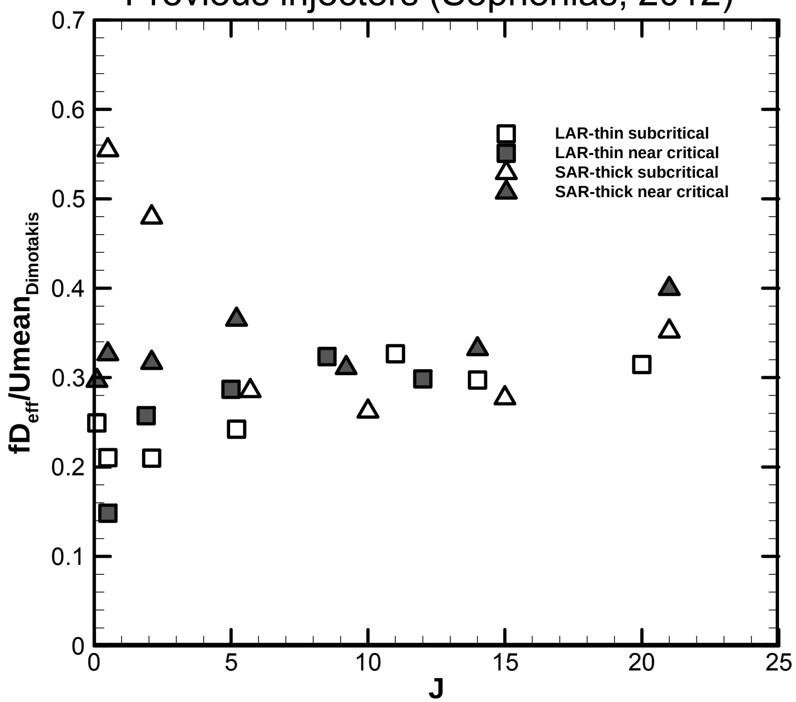

New injector (Wegener, 2013)

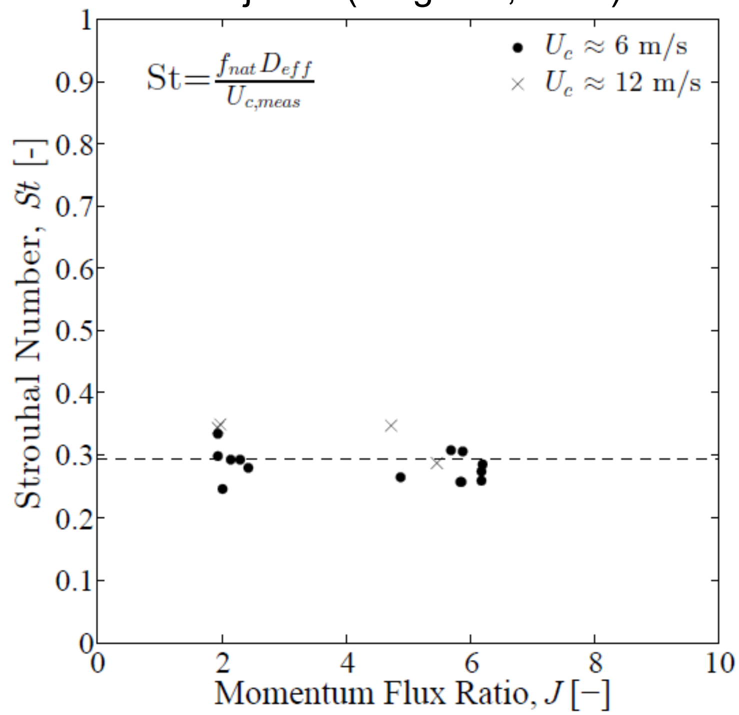

Forced Cases

Representative cases for pressure node and pressure antinode

baseline

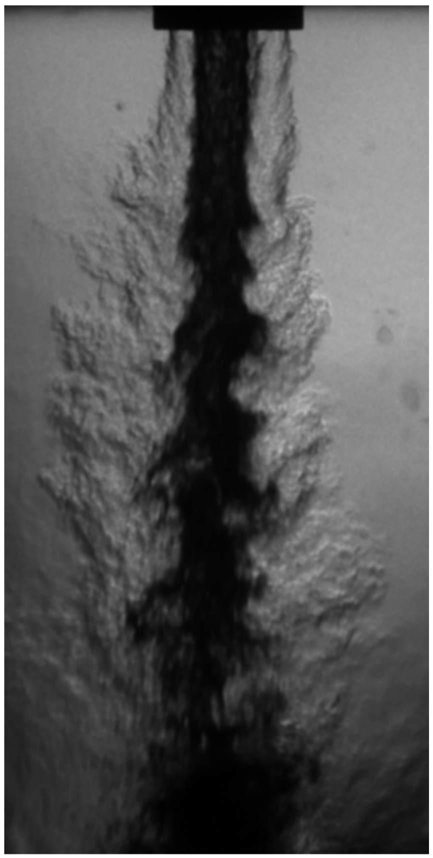

Pressure antinode

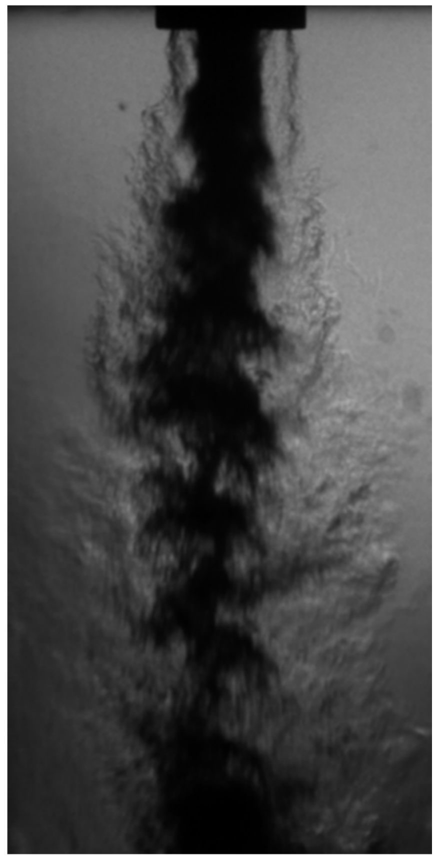

Pressure node

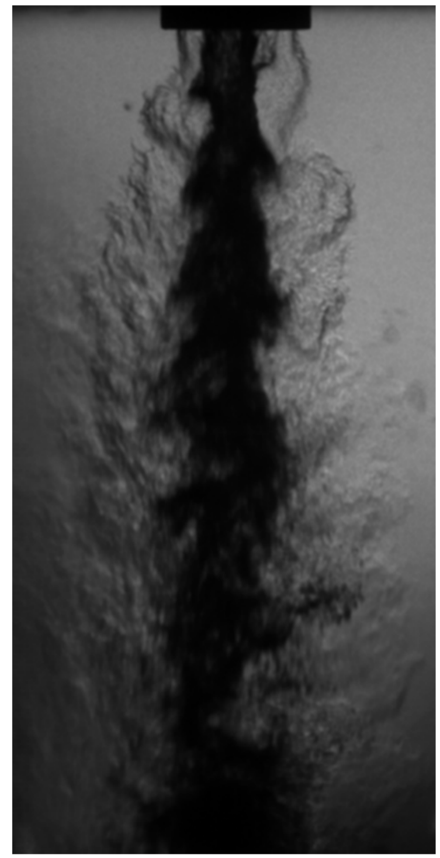

Pressure Antinode Response J = 2

$$A = \frac{p'}{\frac{1}{2}\rho_2 U_2^2}$$

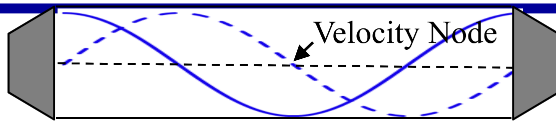

$$F = \frac{f_{forcing}}{f_{jet}} = 2.6$$

0.28 0.44 0.73 1.6 2.49 4.39 4.97

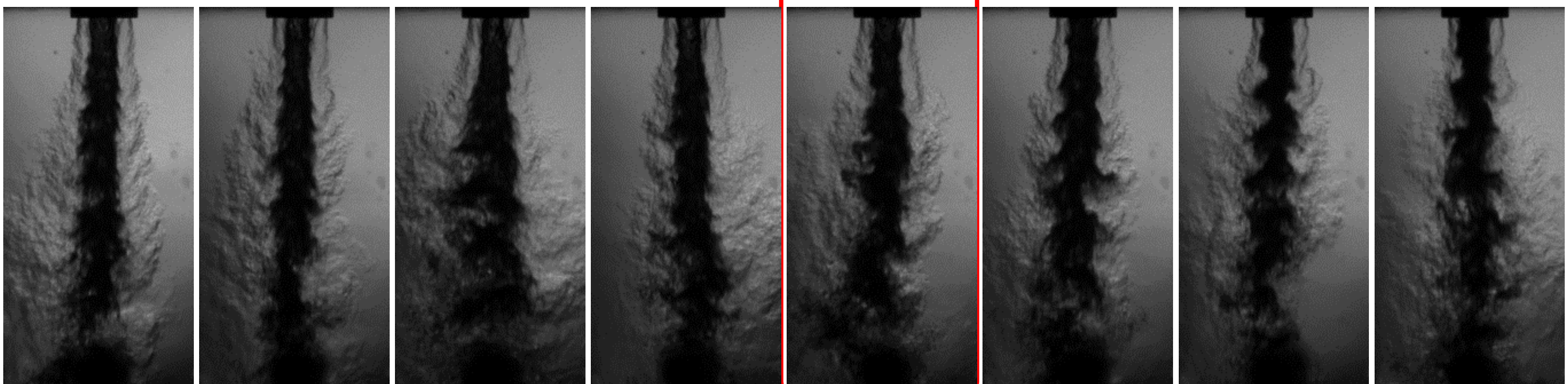

No receptivity

Weak receptivity

High receptivity

Natural convective POD mode pair

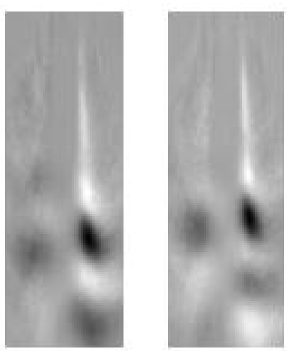

Forced convective POD mode pair

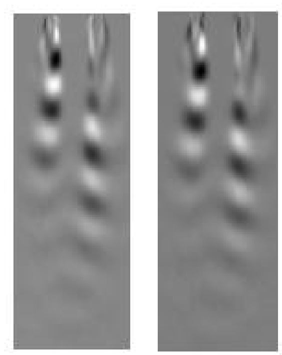

Pressure Antinode Mechanism

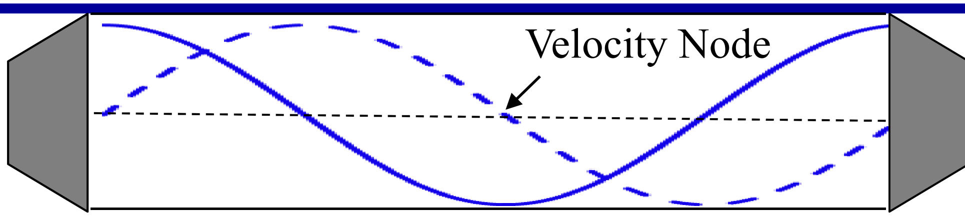

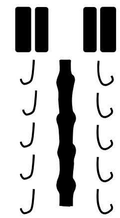

Outer jet mass flow pulsations

POD structure | unforced | Max forcing | POD structure

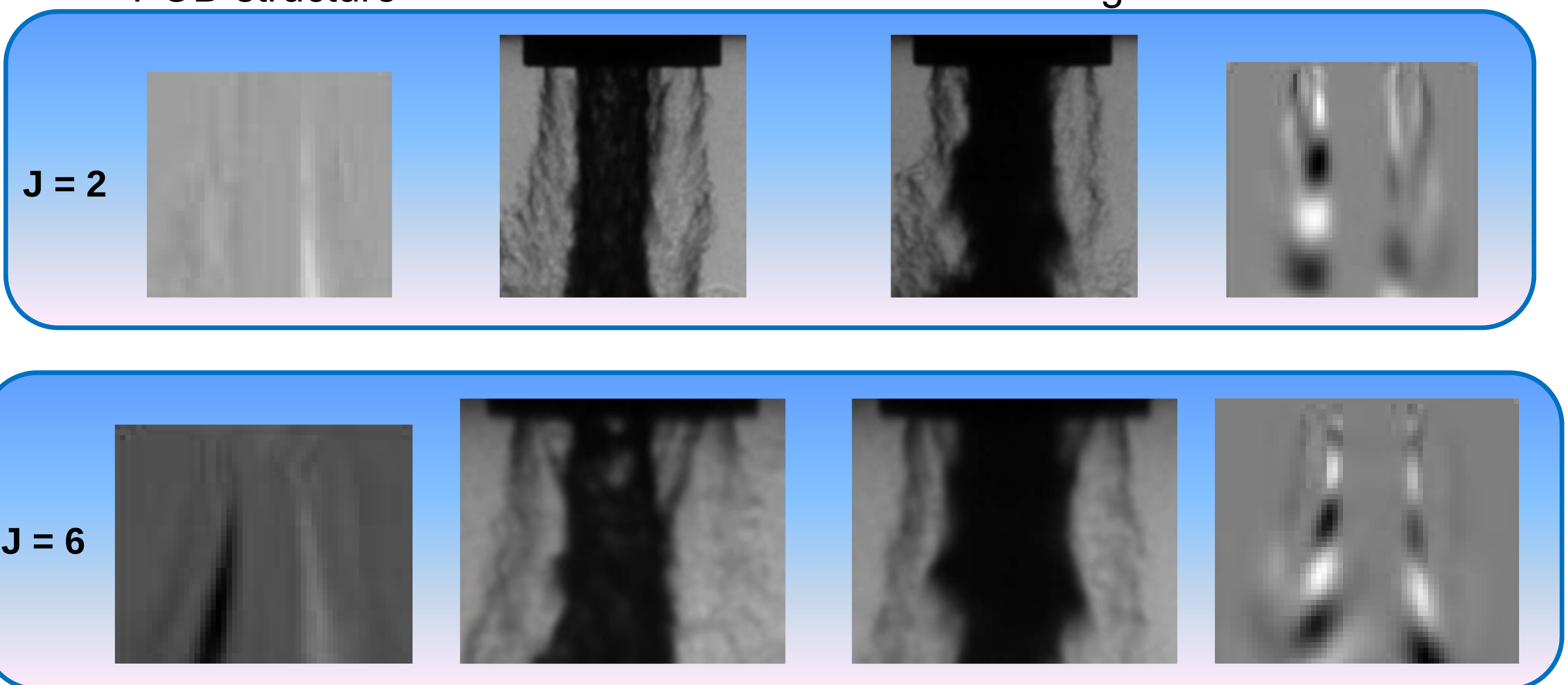

Pressure Node Response J = 2

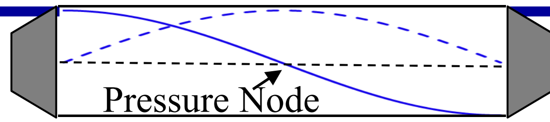

$$F = \frac{f_{forcing}}{f_{jet}} = 2.6$$

U' = 0 | 0.06 m/s | 0.12 m/s | 0.16 m/s | 0.25 m/s | 0.34 m/s | 0.52 m/s | 0.72 m/s

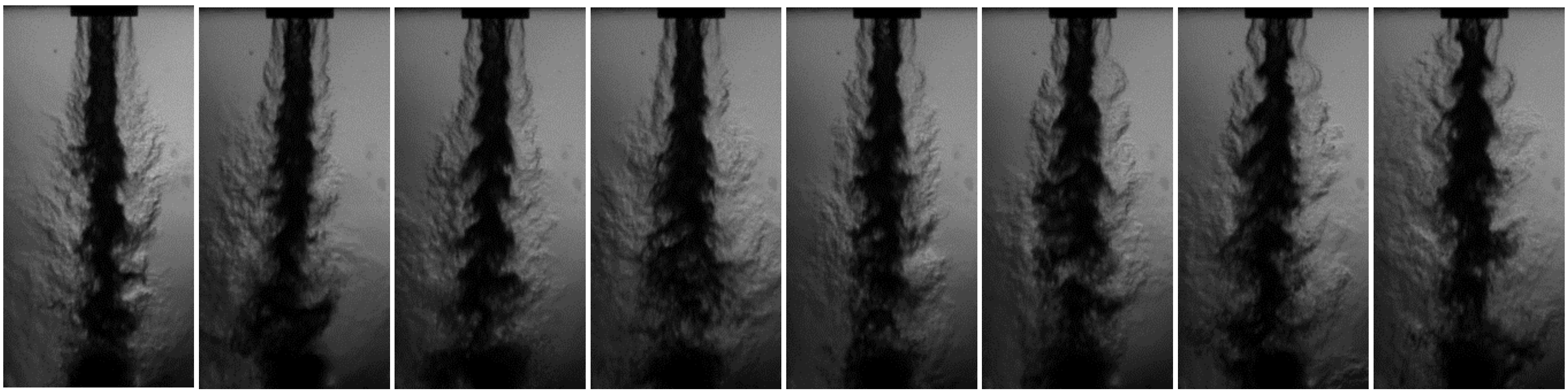

No receptivity

Weak receptivity

High receptivity

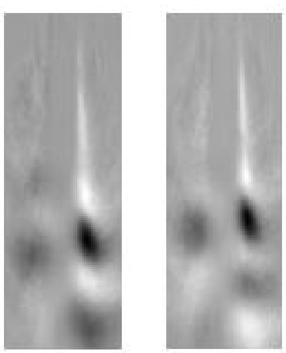

Natural convective POD mode pair

Forced convective POD mode pair

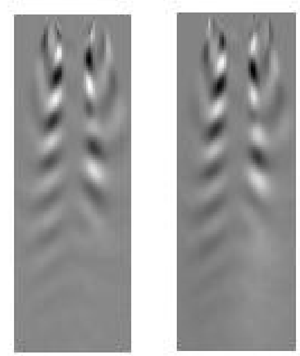

Pressure Node Mechanism

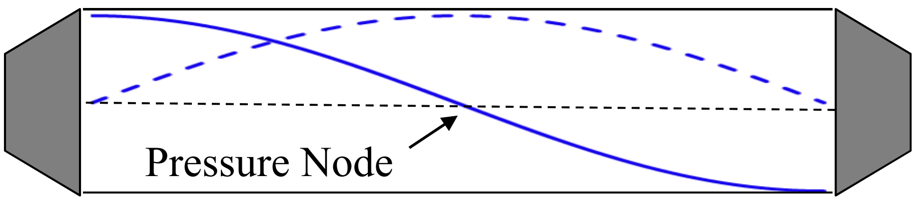

Apparent excitation of antisymmetric mode in the outer jet that drives instabilities in the inner jet

J = 2

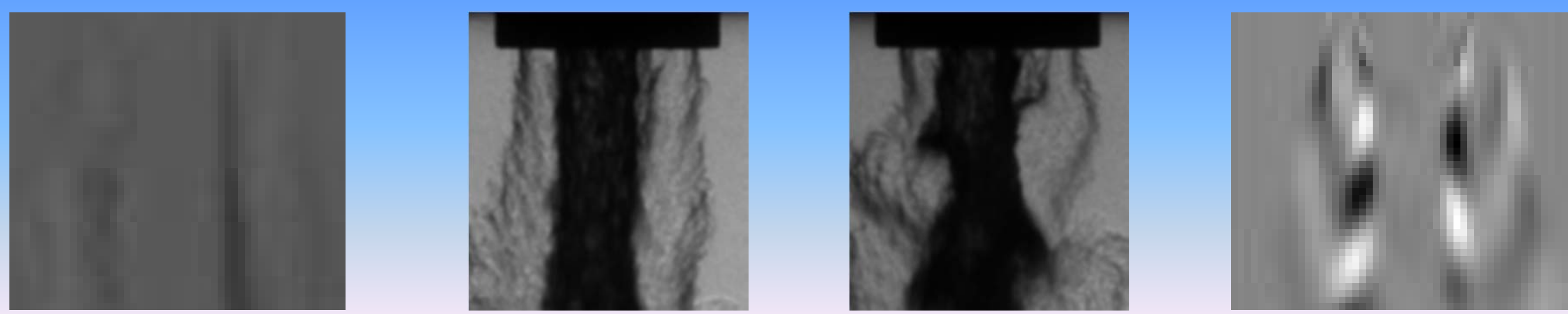

J = 6

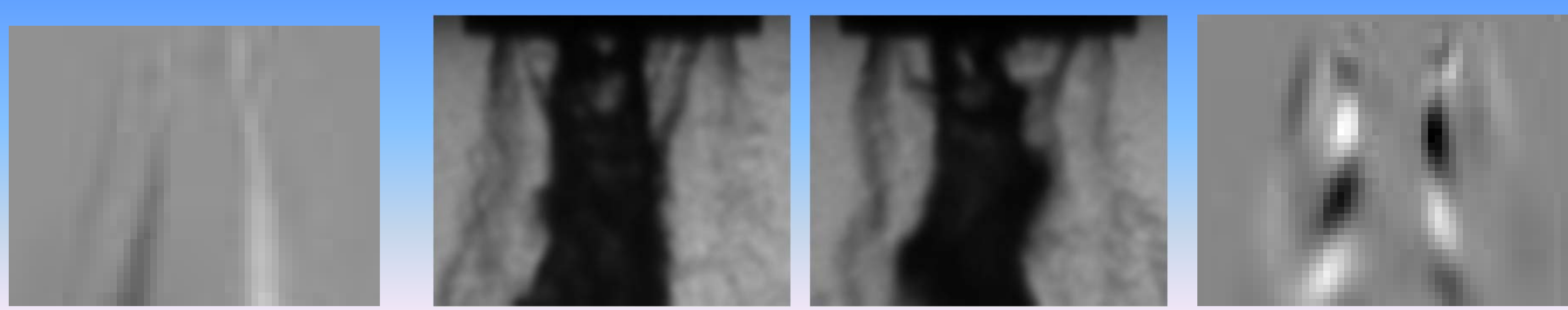

Receptivity

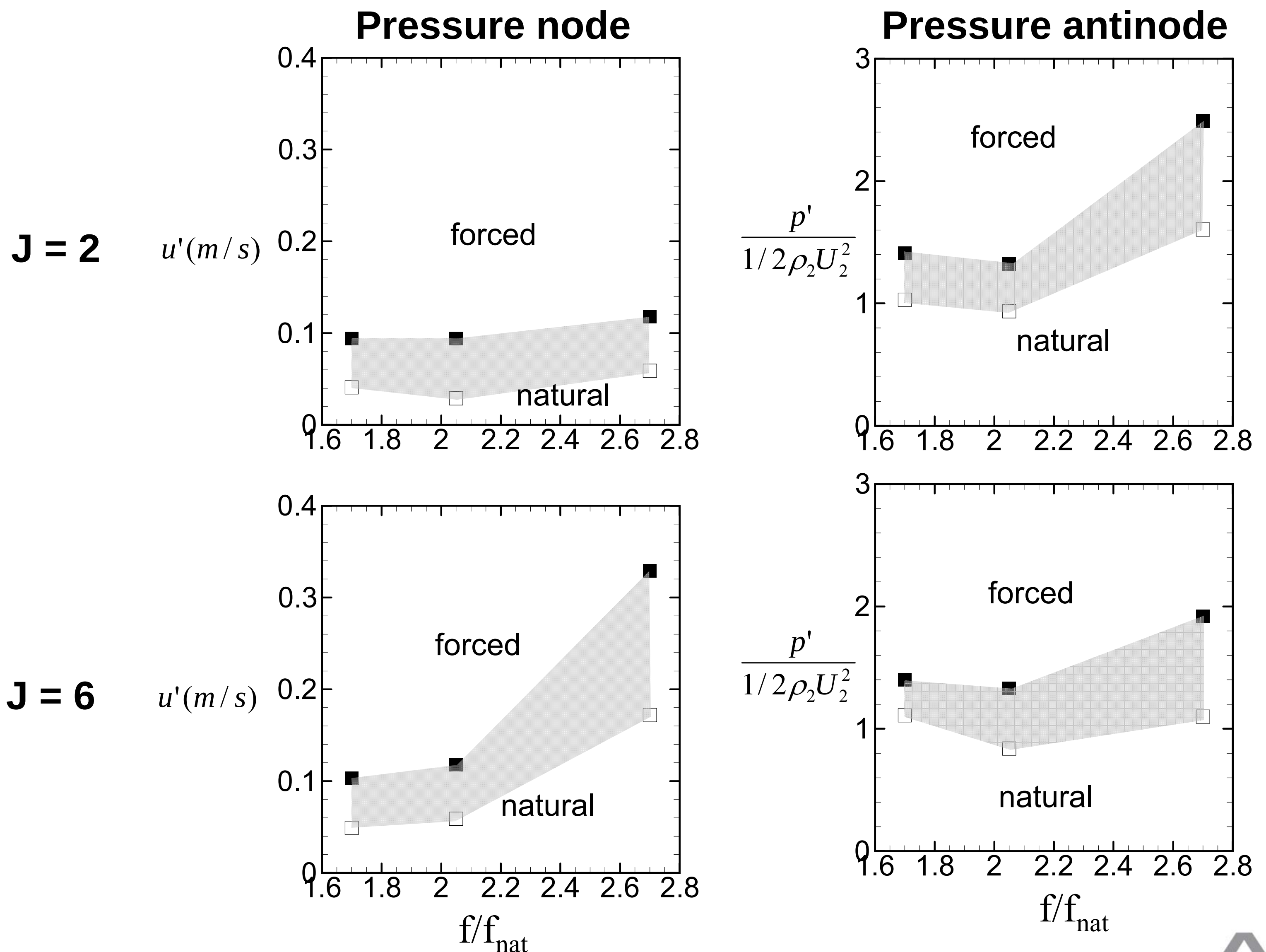

Summary

- **Convection velocity predicted using shear layer model**
- **Coaxial jet preferred mode scaling law**
- **Receptivity characteristics for J = 2 and 6**
  - **Pressure antinode → outer jet puffing mechanism**
  - **Scales with outer jet dynamic pressure**
  - **Pressure node → excitation of helical or antisymmetric mode**
  - **Very sensitive mode—driven by low level forcing**

Future Work

- **Determine robustness of scaling laws**
  - **Convection velocity (i.e. Dimotakis law)**
  - **Strouhal number**
- **Supercritical conditions**
- **Reacting flow conditions**
- **Multiple injectors**

Backup slides

Unforced Coaxial Jets

- **Frequency depends on location**

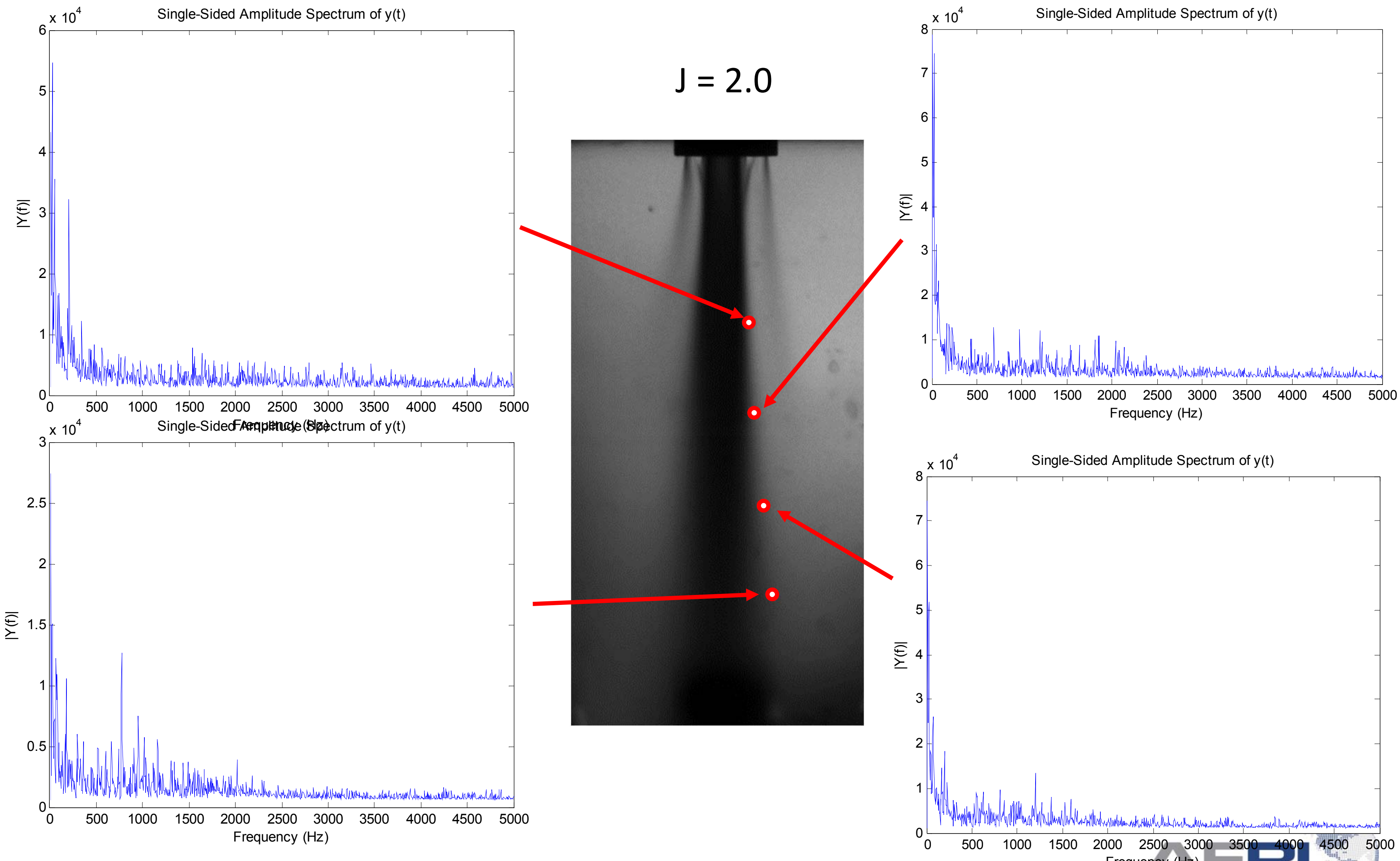

Convection Velocity

Convective Shear Layer Velocity by Dimotakis (1986)
Vortex Frame of Reference

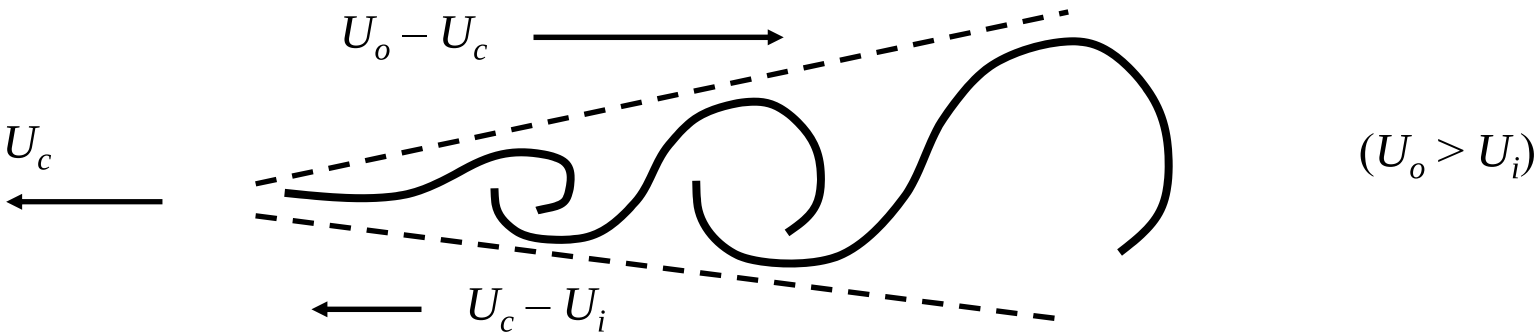

- Bernoulli's equation
  - A stagnation point must exist between vortices. Therefore, along a line through this point, dynamic pressures are approximately equal.

$$\rho_o (U_o - U_c)^2 \approx \rho_i (U_i - U_c)^2$$

$$U_c = \frac{U_o \rho_o^{1/2} + U_i \rho_i^{1/2}}{\rho_o^{1/2} + \rho_i^{1/2}} \qquad St = \frac{f_{nat} D}{U_c}$$

$\Rightarrow$ If *St*, *D*, U_c are held constant then f_{nat} may be constant.

AFRL

Convective Mode from POD

- Proper Orthogonal Decomposition
  - To identify traveling, coherent structures, a conjugate mode pair is identified as any two modes whose CPSD magnitude peaks near a phase of ±90°.[12]

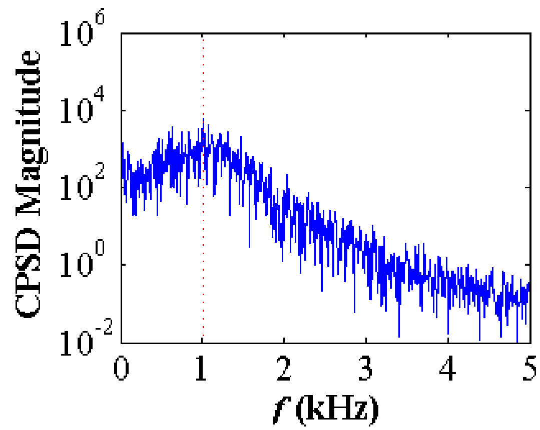

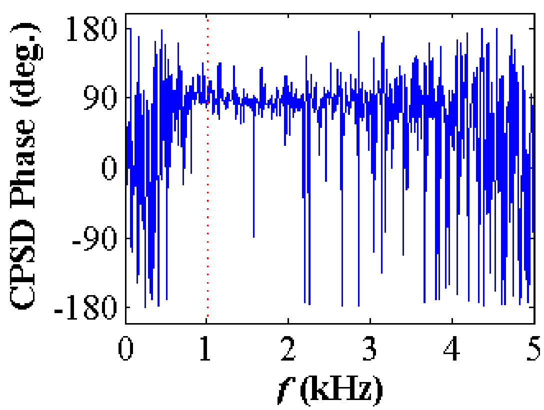

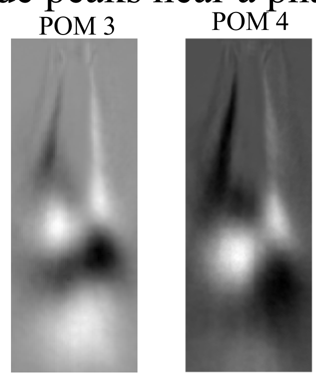

POMs 3 & 4 exhibit the same flow structure, shifted by 90° in the direction of flow.

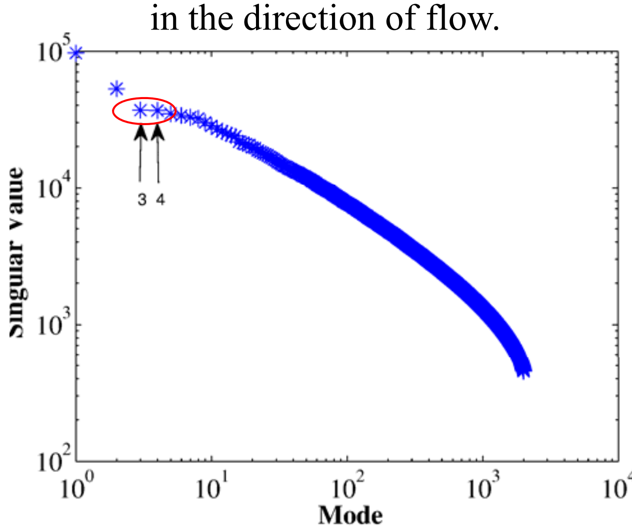

⇒ Proper orthogonal modes (POMs) 3 & 4 were found to be the **most energetic conjugate pair.**

⇒ The natural mode is represented by POMs 3 & 4.

⇒ The natural mode spans a band of frequencies rather than a single peak frequency.

Arienti, M. and Soteriou, M.C.(2009)